

Correlated electron transport assisted by surface acoustic waves in micron-separated quasi-one-dimensional channels

Jian-Hong He,¹ Jie Gao,^{1,2,a)} and Hua-Zhong Guo¹

¹Department of Physics, Sichuan University, Chengdu 610064, People's Republic of China

²National Institute of Measurement and Testing Technology, Chengdu 610021, People's Republic of China

(Received 15 June 2010; accepted 30 August 2010; published online 23 September 2010)

We present the experimental investigation of correlated electron transport through three micron-separated quasi-one-dimensional channels formed in an $\text{Al}_x\text{Ga}_{1-x}\text{As}/\text{GaAs}$ heterostructure. A surface acoustic wave captures electrons from the two-dimensional electron gas and drives them through two depleted channels connected with an open ballistic channel, where different potential situations are defined by three etched gates placed in series. Experimental results show an acoustoelectric current transition with two sets of quantized plateau which demonstrates the electron-electron correlation due to Coulomb interactions. This basic scheme is toward a physical implementation of quantum logic gates and the realization of quantum entanglement. © 2010 American Institute of Physics. [doi:10.1063/1.3491287]

With the availability of intricate nanofabrication technology, charge transport through mesoscopic systems has been extensively studied for the potential applications on nanoelectronics.^{1,2} Surface acoustic waves (SAWs) provide an alternative way to control single-electron dynamics in nanodevices.³⁻⁵ The SAW single electron transport devices were originally investigated in the context of metrological application for defining a type of current standard.³ Recently acoustoelectric current in systems of coupled one-dimensional channels along which a SAW minimum carries electrons has attracted a lot of interest.⁶⁻⁹ Ebbecke *et al.*⁶ proposed an experiment to increase the single-electron acoustoelectric current for metrological purpose, as electrons driven by SAWs in two adjacent channels. Furthermore, such acoustic charge transport devices comprising a network of coupled quantum wires can perform the basic operations needed for quantum computing^{7,8} and observation of coherent single-electron dynamics.⁹ In recent theoretical work, Giavaras *et al.*¹⁰ proposed a scheme to calculate the entanglement of two interacting electrons, while one electron is driven by SAW along a quantum wire and the other electron is bound in the wire.

In this paper, we present a system that demonstrates correlated electron transport as the SAWs minima trap electrons orderly passing through two depleted one-dimensional channels separated by a two-dimensional gas (2DEG) reservoir. The measurement is achieved through opening or closing different channels by controlling their gate voltages. Such experimental technology represents a viable approach for the realization of quantum entanglement¹⁰ and fundamental quantum logic gates.¹¹ The operation device comprises a wet etched mesa with three sections of channels in series and their corresponding gate electrodes, as shown in Fig. 1(a). In the figure, we label the three gates as left gate (LG), center gate (CG), and right gate (RG). When sufficiently large negative voltages are applied to the two of the etched trench gates, two depleted channels are defined which connect three regions of the 2DEG, i.e. source, center reservoir, and drain [Fig. 1(b)].

An important advantage of the multichannel device is that we can measure the acoustoelectric current in each channel separately as the channels have a common source and drain but different channel can be depleted and open individually. This contrasts with the experimental device in Ref. 12, where the two split gates were closely spaced that a single long depleted channel was formed by applying sufficient voltages. Observation of correlated electron transport allows us to determine the modulated acoustoelectric current, which is found to be sensitive to the potential of the different channels. Different potential situations can be achieved by changing corresponding gate voltages in order to address multiple depleted channels with different electron reservoirs. As the gate voltages are swept, an acoustoelectric current transition is distinguished as two different sets of plateaus seem to prevail. The regimes of quantum-mechanical confinement, electron-electron interaction, and tunneling demonstrate modulated acoustoelectric current flow in the multichannel system in the closed-channel regime.

The device was fabricated on a $\text{GaAs}/\text{Al}_{0.3}\text{Ga}_{0.7}\text{As}$ heterostructure with 2DEG situated approximately 80 nm below the surface. The 2DEG density was $3.88 \times 10^{11} \text{ cm}^{-2}$, and the mobility was $1.49 \times 10^5 \text{ cm}^2/\text{V s}$. Sections of two shallow-etched semicircular trenches of radius $5.5 \mu\text{m}$ con-

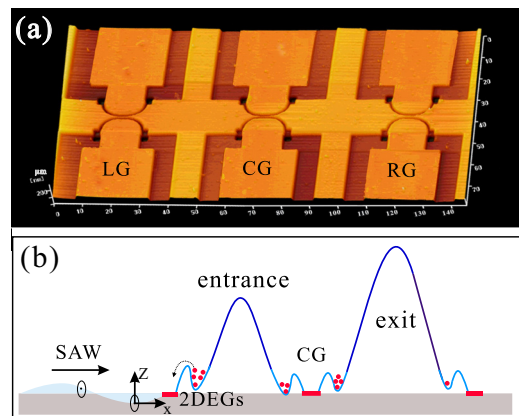


FIG. 1. (Color online) (a) AFM image of etched trench gates. (b) Schematic of simplified experimental layout corresponding (a). The LG and RG define the entrance and exit of the multichannel device.

^{a)}Electronic mail: prof.j.gao@gmail.com.

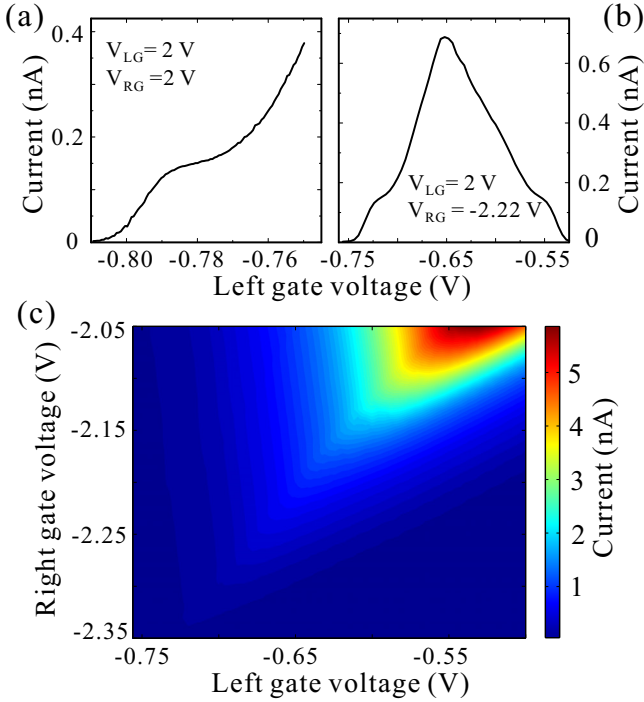


FIG. 2. (Color online) (a) Acoustoelectric current as a function of LG voltage below pinch off voltage. (b) Acoustoelectric current measured for two depleted channels vs V_{LG} , the voltage on RG is -2.22 V. (c) Color-scale plot of acoustoelectric current as a function of V_{LG} and V_{RG} . The applied rf frequency and power are 1007.38 MHz and 17 dBm, respectively.

sisted of a straight segment $2.88 \mu\text{m}$, whereas the large areas of the 2DEG adjacent to the constriction served as gates. An atomic force microscopy (AFM) image of the device with etched trench gates is shown in Fig. 1(a). The width of the three etched gates is $0.8 \mu\text{m}$, $0.5 \mu\text{m}$, and $1.2 \mu\text{m}$, respectively, and the separation between them is $30.2 \mu\text{m}$. The SAW was generated by applying a microwave signal from an Agilent 8648D signal generator to a transducer, made of 100 pairs of interdigitated fingers with a period of $2.88 \mu\text{m}$. Two interdigital transducers (IDTs), facing each other, were deposited 1.16 mm apart on both sides of a 2DEG mesa. The SAW-induced current was measured between the source and drain ohmic contacts using a standard lock-in technique. All measurements were performed in a dilution refrigerator at temperature 0.6 K .

Above all, we separately measure the acoustoelectric current in a single channel in closed-channel regime, and the other two channels are open to conduction. The SAW-induced quantized current displays a plateau at the theoretical value $I = ef$, where e is the electron charge and f is the SAW frequency. Figure 2(a) shows the current as a function of LG voltage below conductance pinch-off. The SAW is launched from the left IDT [see Fig. 1(b)]. Then the voltage on RG is changed to -2.22 V (right channel is completely closed), the pinch-off voltage for the left channel moves positively from -0.81 to -0.75 V since the RG provides additional electrostatic confinement. In particular, the current shows a triangular-shaped peak with quantized current plateau on both sides, as shown in Fig. 2(b). The current shows a maximum around $V_{LG} = -0.65 \text{ V}$, and starts to decrease as V_{LG} is swept more positively. The current through the two depleted channels as a function of V_{LG} and V_{RG} is plotted in color scale in Fig. 2(c), and a highly regular V-shape fan pattern of the transition line is revealed. The peak of V-shaped structure represents the maximum value of current

at corresponding gate voltages. The peak moves to a more negative V_{LG} and the peak value of current decreases when V_{RG} is made more negative.

We now explore the regime of device operations that demonstrates the quantum correlations between electrons due to their mutual Coulomb interactions. Each SAW potential minimum forming a dynamic quantum dot (QD) captures N electrons from the source 2DEG. As the dynamic QD moves through the entrance barrier, the electrons escape from the QD to the source 2DEG by tunneling^{13,14} or by thermal excitation.¹⁵ When the dynamic QD is near the CG, it couples to the open channel acting as a reservoir which is populated with electrons up to the Fermi energy. An exchange of the electrons between the dynamic QD and the reservoir occurs which depends on the size of the confinement and the number of electrons in the QD. The Coulomb repulsion between electrons in the QD leads to an energy cost of the dynamic QD for adding an extra electron into it.¹ The recent observation of few-electron dynamics in experiments of SAW-assisted charge transport¹⁶ revealed that the addition energy of the third electron in each dynamic QD was five times larger than the addition energy of the second one. Therefore, the electron-electron interactions modify the density of states and ultimately the number of electrons in the dynamic QD.

Returning to Fig. 2(b), making V_{LG} more negative from $V_{LG} = -0.525$ to -0.65 V , more electrons escape from the dynamic QD as it moves through the left channel due to the increasing barrier of the LG. This leads to a stronger coupling between the dot and center reservoir and hence to surmount a weaker Coulomb repulsion for adding the electrons to the dot from the center reservoir. In particular, the electrons tunnel from the center reservoir to the left channel is suppressed as the left barrier height increases. Thus, the dynamic QD can recapture more electrons from the center reservoir passing through the right potential barrier. In this case, the measured current increase to a peak of $\sim 700 \text{ pA}$. At deeply pinched-off region from $V_{LG} = -0.65$ to -0.75 V , the variation of the left potential barrier that changes by the LG voltage is rapid compared with the addition energy scales due to the Coulomb interactions. In this regime, the left depleted region lengthens and the potential gradient near the left channel entrance becomes sufficiently large so the current falls to zero.

The detailed structure of the observed acoustoelectric current transitions is better visible in the color-scale plot of the numerical derivative of the current dI/dV_{LG} (Fig. 3). Two zones are distinguished (type A and B) where the zero derivative of dI/dV_{LG} corresponding to two sets of current plateau show different behaviors with respect to V_{LG} and V_{RG} . The dotted transition line with the zero derivative corresponds to the peak of the current. On the left-hand side of the dotted transition line, the set of plateau (type A) changes their position along the V_{RG} -axis. In contrast, another set of plateau (type B) changes their position along the V_{LG} -axis in response to much smaller changes in V_{RG} . Therefore, we identify that the set of plateau (type A) corresponds to the plateau for only the left channel in closed-channel regime [Fig. 2(a)] whereas the appearance of another set of current plateau (type B) arises from the electron-electron correlation. Indeed, the dynamics of the electrons localized in the SAW potential are determined by the long-range Coulomb interaction.¹⁷ The coupling between the bound electrons in

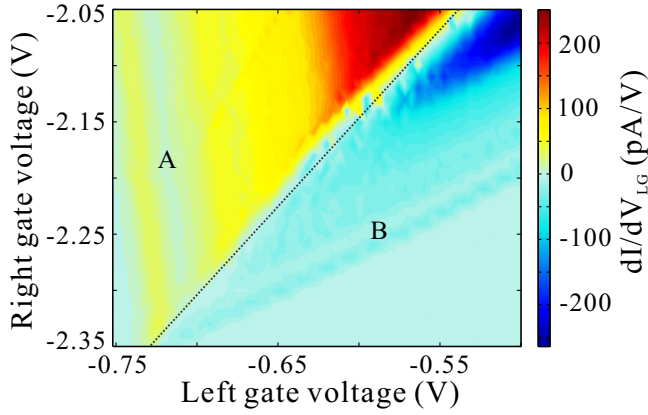


FIG. 3. (Color online) The numerical derivative dI/dV_{LG} of current with respect to V_{LG} and V_{RG} based on the data in Fig. 2(c).

the dynamic QD and the electrons in the entrance of the RG channel leads to a strong building up of quantum correlations. Such electron-electron correlation gives rise to the modulation of energy states of QD (Ref. 18) which contributes to quantized current plateau (type B). It is important to note that the slope of the lines of type A with respect to V_{LG} -axis ($k_{A-LGaxis} \approx 12$) is much larger than the slope of the lines of type B ($k_{B-LGaxis} \approx 0.6$), see Fig. 3. This suggests that the acoustoelectric current on the left-hand side of the peak is very sensitive to the LG potential. Moreover, the ef plateau on the right-hand of the peak is dominated by the RG potential barrier and is indirectly affected by the LG via electron-electron correlation with Coulomb interaction.

To investigate the modulation effect of dynamic potential, we have performed measurements by applying two counterpropagating SAW beams to the multichannel system. The experimental data in Fig. 4(a) show a pronounced influence of the additional SAW beam on the correlated electron transport. The graph presents sinusoidal oscillation of the current on the relative phase difference φ of the two SAW beams. The behavior of this oscillation is consistent with our previous study¹⁹ that two counterpropagating SAWs interfere constructively or destructively depending on the phase difference. The modulated piezoelectric potential changes the total number of electrons of the dynamic QDs leading to the change in the Coulomb interactions. The corresponding color-scale plot of the derivative dI/dV_{LG} versus V_{LG} and φ clearly gives evidence of the modulation effect of the additional SAW beams, as depicted in Fig. 4(b). Interestingly, two sets of zero derivative corresponding to the quantized plateau exist, one of which is clearly pronounced with sinusoidal oscillation, and the other shows opposite oscillation behavior. This could originate from different interference patterns which depend on how SAW beams couple to the barriers and depend on the phase difference of the SAWs field at barriers. Indeed as discussed above, the two sets of quantized plateau are principally dominated by the entrance and exit potential barrier of multichannel system, respectively. In our sample structure, the separation between the LG and RG is approximately $(n+1/2)\lambda$ ($n \approx 30$) which leads to two opposite patterns of interference. As the phase periodically shifts, two sets of oscillation behavior of the acoustoelectric current are expected to occur.

In summary, we have studied the acoustoelectric transport through a multiple quasi-one-dimensional channels system. Two sets of quantized current plateau have been observed when the left and right gate voltages are swept. Our

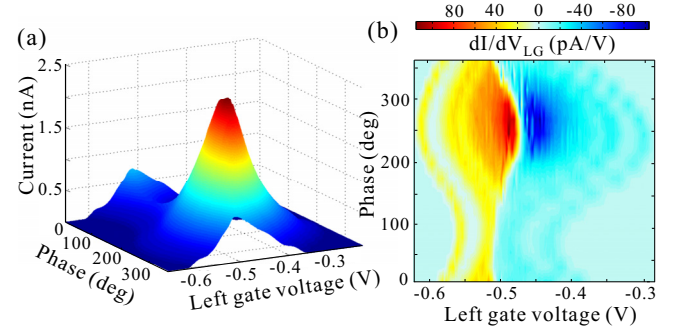


FIG. 4. (Color online) (a) Acoustoelectric current as a function of V_{LG} and phase. The microwave applied to the left IDT is 17 dBm. For the right IDT, this source power is attenuated by 15 dB and the phase is modulated in steps of 24° through a 360° -cycle. The voltage on RG is -1.62 V. (b) The numerical derivative of dI/dV_{LG} of current vs V_{LG} and phase.

measurements indicate that it is possible to correlatively modulate acoustoelectric current in micron-separated channels. These results demonstrate that the acoustoelectric current transitions are strongly sensitive to the spatial potential distribution and make it possible to fabricate complex arrays of gates for microelectronic devices. Furthermore, the work provides great potential for the further study of quantum logic gates and quantum entanglement.

The authors thank P. Utoko, H. Guo, and F. J. Ahlers for useful discussions and their kind help. This research was supported by the Key Program of National Natural Science Foundation of China under Grant No. 60436010 and National Key Technology R&D Program of China under Grant No. 2006BAF06B09.

- ¹L. P. Kouwenhoven, A. T. Johnson, N. C. Van der Vaart, C. J. P. M. Harmars, and C. T. Foxon, *Phys. Rev. Lett.* **67**, 1626 (1991).
- ²S. Datta, *Electronic Transport in Mesoscopic Systems* (Cambridge University Press, Cambridge, England, 1995).
- ³J. M. Shilton, V. I. Talyanskii, M. Pepper, D. A. Ritchie, J. E. F. Frost, C. J. B. Ford, C. G. Smith, and G. A. C. Jones, *J. Phys.: Condens. Matter* **8**, L531 (1996).
- ⁴V. I. Talyanskii, J. M. Shilton, M. Pepper, C. G. Smith, C. J. B. Ford, E. H. Linfield, D. A. Ritchie, and G. A. C. Jones, *Phys. Rev. B* **56**, 15180 (1997).
- ⁵V. I. Talyanskii, J. M. Shilton, J. Cunningham, M. Pepper, C. J. B. Ford, C. G. Smith, E. H. Linfield, D. A. Ritchie, and G. A. C. Jones, *Physica B* **249–251**, 140 (1998).
- ⁶J. Ebbecke, G. Bastian, M. Blöcker, K. Pierz, and F. J. Ahlers, *Appl. Phys. Lett.* **77**, 2601 (2000).
- ⁷C. H. W. Barnes, J. M. Shilton, and A. M. Robinson, *Phys. Rev. B* **62**, 8410 (2000).
- ⁸G. Gumbs and Y. Abranyos, *Phys. Rev. A* **70**, 050302 (2004).
- ⁹M. Kataoka, M. R. Astley, A. L. Thorn, D. K. L. Oi, C. H. W. Barnes, C. J. B. Ford, D. Anderson, G. A. C. Jones, I. Farrer, D. A. Ritchie, and M. Pepper, *Phys. Rev. Lett.* **102**, 156801 (2009).
- ¹⁰G. Giavaras, J. H. Jefferson, A. Ramšak, T. P. Spiller, and C. J. Lambert, *Phys. Rev. B* **74**, 195341 (2006).
- ¹¹A. Bertoni, P. Bordone, R. Brunetti, C. Jacoboni, and S. Regiani, *Phys. Rev. Lett.* **84**, 5912 (2000).
- ¹²M. Kataoka, C. H. W. Barnes, H. E. Beere, D. A. Ritchie, and M. Pepper, *Phys. Rev. B* **74**, 085302 (2006).
- ¹³G. R. A. ĩ zin, G. Gumbs, and M. Pepper, *Phys. Rev. B* **58**, 10589 (1998).
- ¹⁴G. Gumbs, G. R. A. ĩ zin, and M. Pepper, *Phys. Rev. B* **60**, R13954 (1999).
- ¹⁵A. M. Robinson and C. H. W. Barnes, *Phys. Rev. B* **63**, 165418 (2001).
- ¹⁶M. R. Astley, M. Kataoka, C. J. B. Ford, C. H. W. Barnes, D. Anderson, G. A. C. Jones, I. Farrer, D. A. Ritchie, and M. Pepper, *Phys. Rev. Lett.* **99**, 156802 (2007).
- ¹⁷T. Byrnes, P. Recher, N. Y. Kin, S. Utsunomiya, and Y. Yamamoto, *Phys. Rev. Lett.* **99**, 016405 (2007).
- ¹⁸G. Giavaras, *Phys. Rev. B* **81**, 073302 (2010).
- ¹⁹J. H. He, H. Z. Guo, L. Song, W. Zhang, J. Gao, and C. Lu, *Physica B* **405**, 404 (2010).